DMD Fast Forward. Published on July 20, 2005 as doi:10.1124/dmd.104.001040

Physiologically Based Pharmacokinetic Model for Pralmorelin Hydrochloride in Rats

Risa Nasu, Yoichi Kumagai, Hirokuni Kogetsu, Masayuki Tsujimoto, Hisakazu Ohtani and Yasufumi Sawada

Pharmacokinetics Department, Central Research Laboratories, Kaken Pharmaceutical Co., Ltd, Shizuoka, Japan (R.N., Y.K. and H.K.) and Department of Medico-Pharmaceutical Sciences, Graduate School of Pharmaceutical Sciences, Kyushu University, Fukuoka, Japan (M.T., H.O. and Y.S.)

a) Physiologically Based Pharmacokinetic Model of Pralmorelin

b) Corresponding author:

Prof. Yasufumi Sawada

Graduate School of Pharmaceutical Sciences, Kyushu University, 3-1-1 Maidashi, Higashi-Ku, Fukuoka 812-8582, Japan

Tel: +81-92-642-6610

Fax: +81-92-642-6614

E-mail: sawada@phar.kyushu-u.ac.jp

c) The number of text pages; 31

The number of tables; 2

The number of figures; 7

The number of references; 16

The number of words in the *Abstract*; 205

The number of words in the *Introduction*; 350

The number of words in the *Discussion*; 854

d) A list of nonstandard abbreviations

PB-PK; physiologically based pharmacokinetic model
GHRP; growth hormone releasing peptide
GHRH; growth hormone-releasing hormone
GHS-R; growth hormone secretagogue receptor
LC-MS/MS; liquid chromatography – tandem mass spectrometry
AUC; area under the blood concentration-time curve
GFR; glomerular filtration rate
CLint; intrinsic clearance

Abstract

Pralmorelin hydrochloride (Pralmorelin), consisting of six amino acid residues, is a growth hormone-releasing peptide (GHRP). The aim of this study is to analyze the pharmacokinetics of pralmorelin after intravenous bolus administration to rats, and to develop a physiologically based pharmacokinetic (PB-PK) model to describe and predict the concentrations of pralmorelin in blood and tissues. Pralmorelin (3 mg/kg) was administered intravenously to 24 Sprague-Dawley rats. Groups of 3 rats were sacrificed by decapitation at each designated time point (up to 4 h), and plasma and tissues (brain, lung, heart, liver, kidney, small intestine, muscle, adipose and skin) were collected. Bile was also pooled until decapitation. The concentration of pralmorelin in samples was determined by LC-MS/MS. Plasma concentrations of pralmorelin declined rapidly in a biexponential manner. Biliary excretion of pralmorelin was so rapid that 80% of the dose was recovered unchanged in the bile within 1 h after administration. The distribution parameters in each tissue were obtained by using hybrid model and integration plot. They revealed that the distribution of pralmorelin into liver was blood flow-limited, while its distribution was permeability-limited in all other tissues. The PB-PK model developed in this study well described the time courses of pralmorelin concentration in the blood and tissues of rats.

Introduction

Pralmorelin hydrochloride (GHRP-2), a synthetic growth hormone-releasing peptide (GHRP) consisting of six amino acid residues, was developed by C.Y. Bowers of Tulane University (New Orleans, USA) and Kaken Pharmaceutical Co., Ltd. (Tokyo, Japan) (Bowers, 1993). It acts through both the growth hormone secretagogue receptor (GHS-R), which is distinct from hypothalamic GH-releasing hormone (GHRH) receptor, and the ghrelin receptor, and it has been developed as both a diagnostic and a therapeutic agent for growth hormone deficiency. Pralmorelin is rapidly excreted unchanged into the bile from the systemic circulation after intravenous administration to rats.

Recently, various biologically active peptides and their analogues have been considered as drug candidates, including somatostatin analogues (Bauer et al., 1982), endothelin antagonist (Nirei et al., 1993, Nishikibe et al., 1993) and renin inhibitor (Ondetti et al., 1981). These small peptides, consisting of 5-10 amino acid residues, have common characteristics, in that they are rapidly taken up by the liver and most of the dose is subsequently excreted unchanged into the bile (Berelowitz et al., 1978, Cathapermal et al., 1991, Greenfield et al., 1989). Both *in vitro* and *in vivo* studies have demonstrated that active transport systems are involved in the hepatic uptake and biliary excretion of these peptides (Yamada et al., 1997, Kato et al., 1999, Akhteruzzaman et al., 1999). Therefore, pralmorelin may also be excreted by active transport systems. However, few studies have

been conducted to elucidate the *in vivo* tissue distribution properties of small peptides.

Physiologically based pharmacokinetic (PB-PK) models provide a systematic understanding of the pharmacokinetic behavior of drugs based on physiological parameters. PB-PK models are useful for drug development because they are helpful in describing the distribution, excretion and biotransformation of drugs, can provide interspecies scale-up, and enable us to predict the drug concentration profile for any dose and route of administration under various physiological conditions, such as impairment of liver or kidney (Sato et al., 1987, Hosseini-Yeganeh et al., 2002).

The aim of this study is to analyze the distribution of pralmorelin and to establish a PB-PK model well describing the profiles of pralmorelin concentration in the blood and tissues of rats.

Materials and methods

Animals

Adult male Sprague-Dawley rats weighing 208-289 g were purchased from Charles River Japan, Inc. (Kanagawa, Japan), and housed in a temperature-controlled room on a normal 12 h light-dark cycle with free access to food and water. All experimental procedures were consistent with those stipulated in the Kaken Pharmaceutical Co.,LTD. Guide for the Care and Use of Experimental Animals.

Materials

Pralmorelin hydrochloride (D-Alanyl-3-(2-naphthyl)-D-alanyl-L-alanyl-L-tryptophyl-D-phenylalanyl-L-lysinamide dihydrochroride) was synthesized by Fuji Chemical Industries, Ltd. (Toyama, Japan). The chemical structure is shown in Figure 1. [^{3}H]Pralmorelin hydrochloride was purchased from Cambridge Research Biochemicals, Ltd. (Cleveland, UK). The specific activity and chemical purity of [^{3}H]pralmorelin hydrochloride were 5.61 mCi/mg and >97%, respectively. The dosing solution used for all animal studies was prepared by dissolving pralmorelin hydrochloride and [^{3}H]pralmorelin hydrochloride in saline. The internal standard, 2-aminobutyryl-3-(2-naphthyl)-D-alanyl-L-alanyl-L-tryptophyl-D-phenylalanyl-L-lysin amide dihydrochloride, was synthesized by Kaken Pharmaceutical Co., Ltd. All other

reagents were of analytical grade or higher.

Drug Administration and Sample Collection

Under light ether anesthesia, rats were cannulated in the femoral vein, artery and bile duct with silicone rubber and polyethylene tubing, respectively. The rats were used for the experiment at 30-60 min after recovery from anesthesia. Pralmorelin solution (3 mg/kg) was administered *via* the femoral vein cannula as a rapid infusion. Blood samples were withdrawn from the femoral artery at designated times of sacrifice (5, 15 and 30 min and 1, 2 and 4 h). The plasma was separated by centrifugation at 12,000 x g for 3 min and kept frozen at –30˚C until analysis. For tissue sampling, the rats were sacrificed by decapitation at designated times, and the brain, lungs, heart, liver, small intestine, kidneys, muscle, adipose and skin were quickly excised. Bile was pooled until sacrifice. Once dissected, the heart was cut open and residual blood was removed. The contents of the small intestine were removed and the tissue was washed with ice-cold saline. All tissues except for the adipose tissue and skin were homogenized in 5 volumes of purified water. The adipose and skin were minced with scissors. All tissues were kept frozen at –30˚C until analysis.

Quantitative Analysis of Pralmorelin

DMD Fast Forward. Published on July 20, 2005 as DOI: 10.1124/dmd.104.001040
This article has not been copyedited and formatted. The final version may differ from this version.

Pralmorelin was analyzed by LC-MS/MS. Plasma was spiked with the internal standard, 25% Block Ace (Dainippon Pharmaceutical Co., Ltd.) and 0.1 M phosphate buffer (pH 6.0) and vortexed. Empore™ Disk plates (96-well, MPC-SD) were used for extracting pralmorelin from rat plasma. Plates were first conditioned with methanol followed by 0.1 M phosphate buffer. Following the sample loading step, the analytes were eluted with 4% ammonia solution/methanol. Samples were dried and then reconstituted in mobile phase (0.1% formic acid : 0.1% formic acid/acetonitrile , 80:20, v/v). The injection volume was 10 μL.

For analysis of pralmorelin in the tissues, samples were extracted with methanol and solid-phase cartridges. Briefly, tissue homogenate aliquots except for the adipose tissue and skin were spiked with the internal standard, 25% Block Ace and 1% TFA/methanol, vortexed and centrifuged. The supernatant was evaporated. The concentrate was dissolved in 25% Block Ace and 0.1 M phosphate buffer and centrifuged. The aqueous phase was applied to solid-phase cartridges for extraction of pralmorelin. The minced adipose and skin tissues were spiked with internal standard and 1% TFA/methanol, vortexed and centrifuged. The supernatant was evaporated. The concentrate was dissolved in 25% Block Ace and 0.1 M phosphate buffer. The samples were applied to solid-phase cartridges for extraction of pralmorelin. The eluate was evaporated and then dissolved in the mobile phase. Aliquots (10 μL) were assayed prior to LC-MS/MS.

LC-MS/MS analysis was performed on a TSQ Quantum tandem mass spectrometer (Thermo Electron Corporation, USA) equipped with a Nanospace SI-2 HPLC apparatus (Shiseido Co., Ltd., Japan). The positive ion mode was used. Selected reaction monitoring using precursor—›product ion combinations of m/z 410—›170 and 417—›170 was used for quantification of pralmorelin and the internal standard, respectively. The analytical column was a 5 μm, 2.1x50 mm PLRP-S reverse polymer column (Polymer Laboratories Ltd., UK).

Estimation of Distribution Parameters

All the plasma concentration data were converted to blood concentrations using equation 1.

$$Ca = R_B \bullet Cp \qquad (1)$$

where Ca, Cp and R_B are the arterial blood concentration, plasma concentration and blood-to-plasma concentration ratio (R_B=0.67).

With regard to the tissue distribution of pralmorelin, we assumed a two-compartment model, which consists of a compartment in rapid equilibrium with blood (“rapid compartment”) and a deep compartment in slow equilibrium with blood. Figure 2 is the schematic representation of a one-organ model for a non-eliminating organ, which describes the distribution of a drug (Sato et al., 1987). Each tissue consists of the capillary

bed and 2 distinct compartments. The first is a blood flow-limited compartment (the rapid compartment) that is in rapid equilibrium with the drug concentration in the blood, i.e., the concentration (Cb) in the capillary bed. In addition, the sum of the distribution volume of the blood flow-limited compartment and the volume of the capillary bed (i.e., the distribution volume rapid compartment) can be described as the product (Kp_0•Vwt) of Kp_0 and the tissue weight (Vwt). The other is the compartment in which the distribution is membrane permeability-limited (the deep compartment). In the latter compartment, the membrane permeation clearance from the rapid compartment into the deep compartment and the backflux rate constant from the deep compartment into the rapid compartment are represented as PS•fb and k2, respectively.

We defined Kp and Kp_0 as the tissue-to-blood concentration ratio attributable to the drug in the deep compartment and that attributable to the rapid compartment, respectively. Because the Kp values in three early points (5, 15 and 30 min) were constant, the average of these 3 points was regarded as Kp_0.

In addition, hybrid model (Fig. 2) was fitted to tissue concentrations using the arterial blood concentration-time profile to determine PS•fb and k2.

The hepatic uptake of pralmorelin was so rapid that we could not estimate the PS•fb and k2 values. Therefore, we designed another *in vivo* hepatic uptake study, as described in the following section.

To investigate the nature of rapid compartment, we attempted to compare the estimated Kp_0 value with the Kp value of inulin, a marker of extracellular space. Unfortunately, the Kp value of inulin was not available, so that we compared the tissue-to-plasma concentration ratio (Kp,plasma) of inulin at 5 min with that of pralmorelin instead. Furthermore, we regarded the Kp,plasma value at 5 min as the distribution into the rapid compartment. We measured the Kp,plasma values at 5 min after intravenous administration of pralmorelin at a dose of 3 mg/kg and [^{3}H]pralmorelin at a dose of 100 μg/kg and compared with that of inulin previously reported by Yamada et al. (1997).

Analysis of Initial Hepatic Uptake after Administration of [^{3}H]Pralmorelin

Under pentobarbital sodium (50 mg/kg, i.p.) anesthesia, the femoral vein and artery were cannulated. [^{3}H]Pralmorelin solution (3.23 μCi, 100 μg/kg) was administered through the femoral vein, and blood samples were collected at intervals of 10-30 s, prior to and at the time of sacrifice. At designated times 30 s - 3 min after administration, the rats were sacrificed, the liver was excised, and a portion of the tissue was weighed and counted for radioactivity. When a tracer amount of pralmorelin was given intravenously and liver uptake was measured within a period short enough to disregard the backflux and biliary excretion of the parent drug and metabolites from the liver, the liver uptake rate of

DMD Fast Forward. Published on July 20, 2005 as DOI: 10.1124/dmd.104.001040
This article has not been copyedited and formatted. The final version may differ from this version.

pralmorelin can be described by the following differential equation

$$\frac{dXt}{dt} = K1 \bullet Ca \qquad (2)$$

Integration of equation 2 and division by Ca gives the following equation 3.

$$Kp(t) = \frac{K1 \bullet AUC(t)}{Ca} \qquad (3)$$

The uptake clearance of the tissue, K1, was obtained from the initial slope of a plot of Kp (mL/g tissue) versus AUC(t)/Ca(t) (min) (Yamazaki et al., 1993).

The uptake clearance of the tissue (K1) was a hybrid parameter of PS•fb (the membrane permeation clearance) and blood flow (Qt). In the liver, we assumed that: 1) each compartment constituting a whole organ is well stirred (well-stirred model), 2) only unbound pralmorelin can diffuse across the membrane into each tissue, 3) only unbound pralmorelin is subject to metabolism and elimination, 4) binding equilibrium of pralmorelin and the distribution into blood cells are rapid enough so that the processes of binding to and dissociation from blood cells are not rate-determining.

Based on the above assumptions, the relationship between the uptake clearance of the tissue (K1; mL/min/g tissue) and the membrane permeation clearance (PS•fb; mL/min) is given by equation 4.

$$K1 \bullet Vwt = \frac{Qt \bullet fb \bullet PS}{Qt + fb \bullet PS} \qquad (4)$$

Therefore, PS•fb is expressed as follows.

$$PS \bullet fb = \frac{K1 \bullet Vwt \bullet Qt}{Qt - K1 \bullet Vwt} \qquad (5)$$

Development of PB-PK Model

Figure 3 represents the developed PB-PK model for the distribution and excretion of pralmorelin in rats. The model consists of 9 tissues and blood compartments that reflect real organs or anatomic tissues in rats. These tissues are connected in parallel between the arterial and venous circulations in this PB-PK model. The blood flows from the venous pool *via* the pulmonary artery into the lung and then out *via* the pulmonary vein into the arterial pool. Except for the liver and lung, all tissues are supplied from the arterial circulation and blood coming out of these tissues flows directly into the venous circulation. The liver receives its blood supply from both the hepatic artery and portal vein. In this model, pralmorelin was assumed to be eliminated only by the liver and kidney, but not by other tissues.

In the liver, the distribution of pralmorelin was rapid and is assumed to be blood flow-limited.

The mass balance equations for the PB-PK model are shown in the Appendix. The equations were integrated numerically and simultaneously using a Macintosh G4 (Apple Computer, Inc. California, USA) with MLAB (Civilized Software, Bethesda, MD, USA).

Results

Total and Hepatic Clearance of Pralmorelin

Plasma concentrations of pralmorelin declined quickly in a biexponential manner after intravenous administration. Pralmorelin was excreted into the bile very rapidly, and 80% of the dose was recovered in the bile within 1 h. The distribution volumes of pralmorelin were small for the skin, adipose, muscle, brain and heart, and large for the liver and kidney.

For analysis, all plasma data were converted to blood concentrations by means of equation 1.

The total blood clearance of pralmorelin was 419 mL/hr. Since previous studies have reported that almost 80% of the dose of pralmorelin is excreted unchanged into the bile, and 8% of the dose is excreted into urine within 24 h after intravenous administration, we assumed that 8% of the dose was eliminated by the kidney and the rest was assigned to the liver in this study. Consequently, the hepatic and renal blood clearances were calculated as 382 and 36.9 mL/hr, respectively. Renal blood clearance is almost equal to the product of the glomerular filtration rate (GFR; 245mL/hr; Yamada et al., 1997) and fb of pralmorelin (0.129). Therefore we assumed that pralmorelin was not subject to renal secretion/reabsorption and the renal clearance was accounted for only by glomerular filtration. The hepatic blood clearance was converted to the hepatic intrinsic clearance

DMD Fast Forward. Published on July 20, 2005 as DOI: 10.1124/dmd.104.001040
This article has not been copyedited and formatted. The final version may differ from this version.

($CLint_H$) by equation 6 based on a "well-stirred" model.

$$fb \bullet CL\,\mathrm{int}_H = \frac{CL_H \bullet Q_H}{Q_H - CL_H} \qquad (6)$$

The hepatic intrinsic clearance was calculated to be 830 mL/hr.

Estimation of Distribution Prameters

Kp_0 values were determined from the average of Kp values in three early sampling points. Kp_0 and PS•fb were estimated from fitting the arterial blood concentration-time profile to the tissue concentrations. Kp. Kp_0, PS•fb and k2 are presented in Table 1.

To determine whether the estimated Kp_0 value is consistent with the vascular volume in tissue, the tissue-to-plasma concentration ratio (Kp,plasma) of pralmorelin at 5min after intravenous administration was compared with that of inulin. Figure 4 shows that the relationship between the Kp,plasma of inulin and pralmorelin (100 μg/kg and 3 mg/kg) at 5 min after intravenous bolus administration in rats was linear ($y = 1.20x$; $r = 0.775$, $p < 0.05$).

Analysis of Initial Hepatic Uptake after Administration of [^{3}H]Pralmorelin

The time profiles of [^{3}H]pralmorelin concentrations in the blood and liver within short period after administration were investigated to estimate the initial hepatic uptake. The Kp and AUC/Ca were plotted in Figure 5 based on equation 3. The slope (K1) was linear

up to 3 min after intravenous bolus administration (Fig. 5). The hepatic uptake clearance (K1) of [^{3}H]pralmorelin was thus calculated to be 1.15 mL/min/g liver.

In the liver, the PS•fb was calculated according to equation 5 using K1 based on a "well-stirred" model. The calculated PS•fb (99.7 mL/min) was sufficiently larger than Q_H (11.8 mL/min). Thus, the distribution of pralmorelin into the liver was considered to be blood flow-limited. The Kpss value in the liver was determined by curve-fitting using a hybrid model with the arterial blood concentration-time profile as the input function (Hosseini-Yeganeh et al., 2001). The estimated Kpss value for the liver was 18.9 (Table 2).

PB-PK Modeling

Distribution into all tissues except for the liver was considered to be membrane permeability-limited, because the PS•fb values were much lower than the blood flow rate.

Physiological parameters reported for a 250-g rat (Hosseini-Yeganeh et al., 2002) and the estimated parameters are listed in Table 1 and 2.

Figures 6 and 7 show the simulated concentration-time profiles of pralmorelin along with the observed concentration-time data for blood and tissues after intravenous administration of pralmorelin (3 mg/kg). The developed PB-PK model agreed well with the observed concentrations in blood and tissues over 4 h, indicating that the developed

PB-PK model is appropriate to describe the kinetics of pralmorelin.

Discussion

Pralmorelin is rapidly eliminated from the body via the hepatobiliary route in rats. To clarify the determinant factors of the pharmacokinetics of pralmorelin, we analyzed the tissue distribution profile of pralmorelin using a PB-PK model, which enabled us to predict the profile of the drug concentration in each tissue from that in the blood.

The Kp_0 value represents the tissue-to-blood concentration ratio attributable to the drug in the rapid compartment (distribution volume that consists of the blood space and the volume in rapid equilibrium with blood). Kp_0 value often coincides with a fraction of the capillary bed volume in the tissue. However, Kp_0•Vwt in this study were significantly higher than the capillary bed volumes, suggesting that pralmorelin rapidly distributes into the space other than the capillary bed (Fig. 2). Therefore, we compared the Kp,plasma values of pralmorelin at 5 min after intravenous administration with those of inulin, a marker for extracellular space because Kp,plasma value at 5 min is considered to reflect the rapid compartment (Fig. 4). We found that the Kp,plasma values of pralmorelin are linearly correlated with those of inulin for several non-eliminating tissues. Thus, the Kp_0•Vwt reflects the distribution to the capillary bed and extracellular space.

Furthermore, the Kp,plasma (3.91) of pralmorelin for the liver was much higher that of inulin (0.17), while the Kp,plasma(1.82) of pralmorelin for the kidney was lower than that of inulin (9.20; Yamada et al., 1997). The membrane permeation clearance (PS•fb; 99.7

mL/min) into the liver, calculated from the K1 value based on the “well-stirred” model, was far larger than Q_H (11.8 mL/min). Taking into consideration that the distribution of pralmorelin into all tissues except for the liver was membrane permeability-limited, pralmorelin may be taken up into hepatocytes by active transport systems.

On the other hand, the relatively poor distribution of pralmorelin into the kidney may be explained by the difference in the protein binding ratio in blood between pralmorelin and inulin. The unbounded fraction (fb) of inulin in blood is almost 1.0, while that of pralmorelin is very low (0.216). Therefore, the glomerular filtration rate of pralmorelin is much smaller than that of inulin. However, the Kp,plasma (1.82) of pralmorelin for the kidney is still higher than 1. This accumulation in the kidney may be attributable to the binding of pralmorelin, the retention of filtered pralmorelin in the renal tubules, or both (Sato et al., 1987).

In this study, we separately examined the initial hepatic uptake by using [^{3}H]pralmorelin, because the hepatic uptake of pralmorelin was so remarkably rapid, in order to develop the PB-PK model for the liver. As shown in Figures 6 and 7, the concentration of pralmorelin estimated by the PB-PK model agreed well with the observed data. For drugs that are subject to rapid hepatobiliary excretion, the uptake clearance may not be accurately estimated by use of the sampling schedule for other organs. In such a case, it is essential to estimate accurately the hepatic uptake clearance

for developing the PB-PK model.

However, the PB-PK model underestimated the liver in a terminal elimination phase. It may be due to the adsorption of pralmorelin to the endothelium and/or parenchymal cell in the liver. Cationic macromolecules tend to bind electrostatically to the surface of hepatocytes in a non-specific manner (Nishida et al., 1991). As pralmorelin has positive charge at physiological pH, it may be adsorbed electrostatically on the surface of hepatocytes. Indeed, our preliminary experiment using isolated rat hepatocytes indicates that pralmorelin highly binds to the surface of hepatocytes (data not shown). Therefore, the underestimation of pralmorelin concentrations in the liver is conceivably attributable to the adsorption, which provides a compartment with rapid binding and slow dissociation, not described by the present model for the liver with the assumption of rapid equilibrium with blood.

Another possible explanation is the sequestration of pralmorelin into the liver. Since the membrane permeation clearance into the liver was much larger than hepatic blood flow, hepatic distribution of pralmorelin is conceivably attributable to the active transport system, such as transporter or endocytosis, and its passive influx and efflux may be quite limited. Therefore, although pralmorelin taken up into the liver is excreted unchanged into the bile, it may be partially subject to hepatic sequestration.

The concentrations of pralmorelin at 30 min in most tissues were higher than model

simulates. However, the blood concentrations were also slightly increased at the same time. Because the time course of blood concentration was obtained by a one-points-per-animal method, the blood concentration at 30 min might be accidentally increased. Therefore, the aforementioned failure in the simulation of tissue concentration may not be due to the flaw of the model.

In conclusion, we have developed a PB-PK model for pralmorelin in rats. The model agreed well with the observed data. The present study also demonstrated that a blood flow-limited compartment and a membrane permeability-limited compartment can account for the distribution of pralmorelin in all tissues except for the liver, and the former represents the distribution to the capillary bed and interstitial fluid. The uptake of pramorelin into the liver was very rapid, suggesting the existence of active transport systems for pralmorelin in the liver.

References

Akhteruzzaman S, Kato Y, Kouzuki H, Suzuki H, Hisaka A, Stieger B, Meier PJ and Sugiyama Y (1999) Carrier-mediated hepatic uptake of peptidic endothelin antagonists in rats. *J Pharmacol Exp Ther* **290:**1107-15.

Bauer W, Briner U, Doepfner W, Haller R, Huguenin R, Marbach P, Petcher TJ and Pless (1982) SMS 201-995: a very potent and selective octapeptide analogue of somatostatin with prolonged action. *Life Sci* **31:**1133-1140.

Berelowitz M, Kronheim S, Pimstone B and Shapiro B (1978) Somatostatin-like immunoreactivity in rat blood. Characterization, regional differences, and responses to oral and intravenous glucose. *J Clin Invest* **61:**1410-1414.

Bowers CY (1993) GH releasing peptides--structure and kinetics. *J Pediatr Endocrinol* **6:**21-31.

Cathapermal SS, Foegh ML, Rau CS and Ramwell PW (1991) Disposition and tissue distribution of angiopeptin in the rat. *Drug Metab Dispos* **19:**735-739.

Greenfield JC, Cook KJ and O'Leary IA (1989) Disposition, metabolism, and excretion of U-71038, a novel renin inhibitor peptide, in the rat. *Drug Metab Dispos* **17:**518-525.

Hosseini-Yeganeh M and McLachlan AJ (2001) Tissue distribution of terbinafine in rats. *J Pharm Sci* **90:**1817-1828.

Hosseini-Yeganeh M and McLachlan AJ (2002) Physiologically based pharmacokinetic model for terbinafine in rats and humans. *Antimicrob Agents Chemother* **46:**2219-2228.

Kato Y, Akhteruzzaman S, Hisaka A and Sugiyama Y (1999) Hepatobiliary transport governs overall elimination of peptidic endothelin antagonists in rats. *J Pharmacol Exp Ther* **288:**568-574.

Nirei H, Hamada K, Shoubo M, Sogabe K, Notsu Y and Ono T (1993) An endothelin ETA receptor antagonist, FR139317, ameliorates cerebral vasospasm in dogs. *Life Sci* **52:**1869-1874.

Nishida K, Mihara K, Takino T, Nakane S, Takakura Y, Hashida M and Sezaki H (1991)

Hepatic disposition characteristics of electrically charged macromolecules in rat in vivo and in the perfused liver. *Pharm Res* **8:**437-444.

Nishikibe M, Tsuchida S, Okada M, Fukuroda T, Shimamoto K, Yano M, Ishikawa K and Ikemoto F (1993) Antihypertensive effect of a newly synthesized endothelin antagonist, BQ-123, in a genetic hypertensive model. *Life Sci* **52:**717-724.

Ondetti MA and Cushman DW (1981) Inhibition of the renin-angiotensin system. A new approach to the therapy of hypertension. *J Med Chem* **24:**355-361.

Sato H, Sugiyama Y, Sawada Y, Iga T and Hanano M (1987) Physiologically based pharmacokinetics of radioiodinated human beta-endorphin in rats. An application of the capillary membrane-limited model. *Drug Metab Dispos* **15:**540-550.

Yamada T, Niinuma K, Lemaire M, Terasaki T and Sugiyama Y (1997) Carrier-mediated hepatic uptake of the cationic cyclopeptide, octreotide, in rats. Comparison between in vivo and in vitro. *Drug Metab Dispos* **25:**536-543.

Yamazaki M, Suzuki H, Hanano M, Tokui T, Komai T and Sugiyama Y (1993)

$Na^{(+)}$-independent multispecific anion transporter mediates active transport of pravastatin into rat liver. *Am J Physiol* **264:**G36-44.

Footnotes

Present address: Laboratory of Drug Informatics, Graduate School of Pharmaceutical Sciences,The University of Tokyo, Hongo, Tokyo, Japan (H.O. and Y.S.)

Legends for Figures

Fig. 1 Chemical structure of Pralmorelin hydrochloride

Fig. 2 Schematic representation of a one-organ model for a non-eliminating organ. Indicated are the blood flow (Qt), the arterial blood concentration (Ca), the concentration in the capillary bed (Cb), the tissue concentration (Ct), the tissue weight (Vwt), the membrane diffusion intrinsic clearance (PS•fb), the backflux rate constant (k2) and the distribution volume that consists of blood space and the space in which the drug concentration rapidly equibrates with blood (Kp_0•Vwt).

Fig. 3 A schematic representation of the PB-PK model to predict the time profiles of pralmorelin concentrations. The arrows show the direction of blood flow. Indicated are the blood flows (Q) of the lung (LU), heart (HE), muscle (MU), skin (SK), liver (H), gut (GU), kidney (R), brain (BR) and adipose tissue (AD), and the intrinsic clearance (CL).

Fig. 4 Relationship between the Kp,plasma values at 5 min after intravenous administration of inulin and pralmorelin. The open circles and closed circles indicate the Kp,plasma values of 100 μg/kg [^{3}H] pralmorelin and those of 3 mg/kg pralmorelin, respectively. The Kp,plasma values of inulin are cited from *Drug Metab Dispos* 25,

536-543, 1997. The solid and broken lines indicate the regression line and 1:1 correlation, respectively. The regression line is $y = 1.20x$ ($r = 0.775$, $p < 0.05$).

Fig. 5 Integration plot for pralmorelin in rat liver. The initial slope represents the K1 value for rat liver (K1 = 1.15 mL/min/g liver).

Fig. 6 Concentration-time profiles for pralmorelin in rat blood and liver after administration of pralmorelin at a dose of 3 mg/kg (i.v.). The symbols represent experimentally observed concentrations and the solid lines are the simulated concentration profiles using the PB-PK model (n = 3, mean ± S.D.). Concentrations-time profiles in semilogarithmic form show in insets.

Fig. 7 Concentration-time profiles for pralmorelin in rat tissues after administration of pralmorelin at a dose of 3 mg/kg (i.v.). The symbols represent experimentally observed concentrations and the solid lines show the simulated concentration profiles using the PB-PK model (n = 3, mean ± S.D.). Concentrations-time profiles in semilogarithmic form show in insets.

DMD Fast Forward. Published on July 20, 2005 as DOI: 10.1124/dmd.104.001040
This article has not been copyedited and formatted. The final version may differ from this version.

Table 1 Distribution parameters for pralmorelin in rats estimated from hybrid model (n = 3, estimates ± error)

Tissue	Kp_0 [a)]	PS•fb [b)]	k2 [b)]
	mL/g tissue	mL/hr	hr^{-1}
Muscle	0.147	2.85 ± 3.93	0.509 ± 1.57
Heart	0.401	0.188 ± 0.180	1.22 ± 2.26
Small intestine	0.835	2.84 ± 4.11	0.718 ± 2.03
Lung	1.06	0.786 ± 0.696	0.313 ± 0.746
Kidney	3.82	2.21 ± 1.72	0.749 ± 0.349
Liver	–	–	–
Brain	0.0397	0.0179 ± 0.0150	0.509 ±0.978
Skin	0.487	1.72 ± 1.23	0.409 ± 0.271
Adipose	0.142	0.337 ± 0.624	0.961 ± 3.34

a) The average of Kp values at 5, 15 and 30min.

b) Estimated from a hybrid model using the blood concentration vs. time curve as the input function.

DMD Fast Forward. Published on July 20, 2005 as DOI: 10.1124/dmd.104.001040
This article has not been copyedited and formatted. The final version may differ from this version.

Table 2 Physiological data and estimated parameters of pralmorelin for various tissues in rats

Tissue	Tissue weght (Vwt)[a)]	Tissue blood flow[a)]	CLint[b)]	Kpss[c)]
	g	mL/hr	mL/hr	mL/g tissue
Arterial blood	5.6	2394	–	–
Venous blood	11.3	–	–	–
Muscle	122	450	–	–
Heart	1	234	–	–
Small intestine	11.4	450	–	–
Lung	2.1	2394	–	–
Kidney	4	552	36.9	–
Liver	10	708	830	18.9
Brain	1.2	78	–	–
Skin	40	348	–	–
Adipose	10	24	–	–

a) The volume and blood flow for each tissue were taken from *Antimicrob Agents Chemother* 46. 2219-2228.2002. The tissue volume was converted to tissue weight based on the assumption of the tissue gravity of 1 g/mL.

b) CLtot is estimated using blood concentration and the renal blood clearance is calculated from the urinary excretion. The extrarenal clearance is assumed as the hepatic blood clearance and calculated using the blood flow. Renal blood clearance is assumed to be equal to the glomerular filtration rate.

c) Estimated from a hybrid model using the blood concentration vs. time curve as the input function.

DMD Fast Forward. Published on July 20, 2005 as DOI: 10.1124/dmd.104.001040
This article has not been copyedited and formatted. The final version may differ from this version.

Fig.1

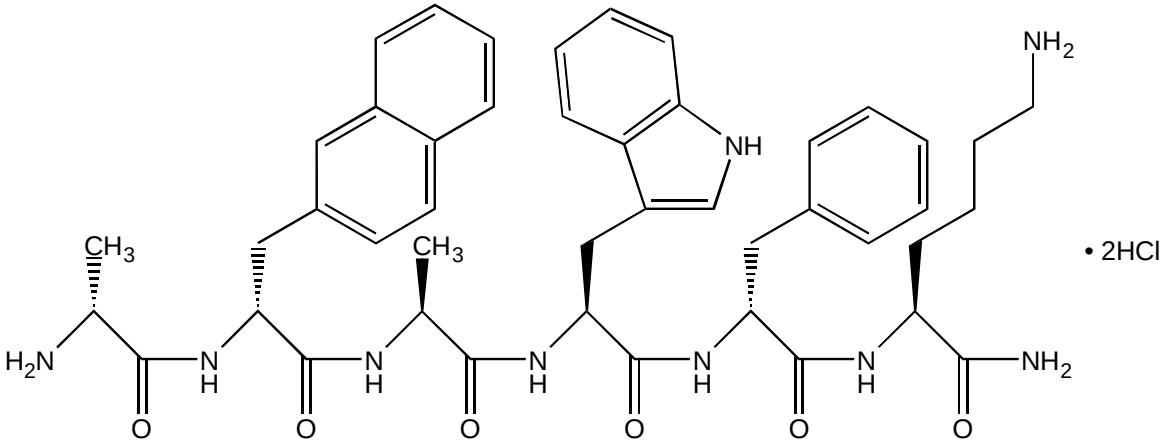

DMD Fast Forward. Published on July 20, 2005 as DOI: 10.1124/dmd.104.001040
This article has not been copyedited and formatted. The final version may differ from this version.

Fig.2

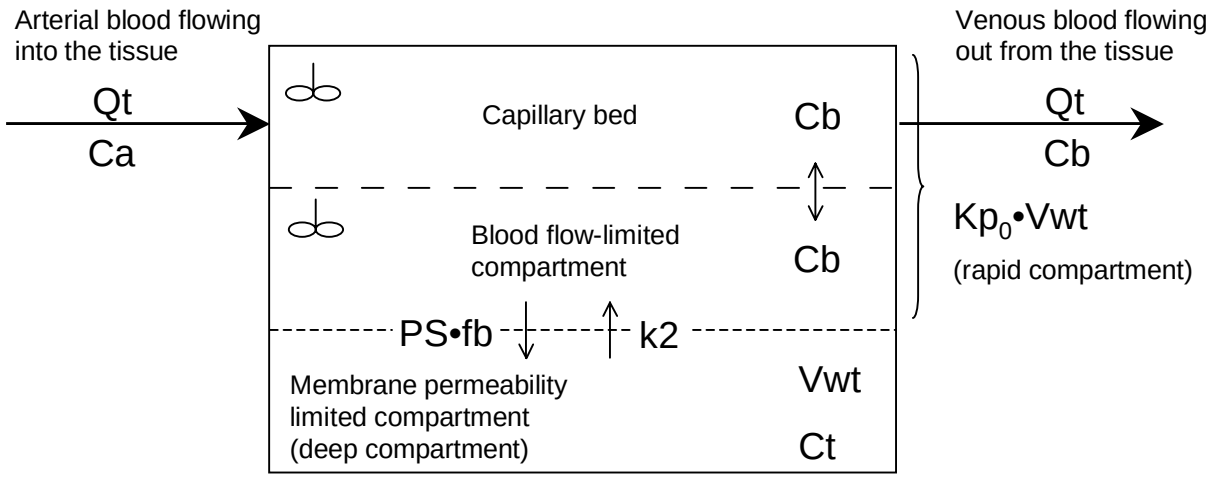

DMD Fast Forward. Published on July 20, 2005 as DOI: 10.1124/dmd.104.001040
This article has not been copyedited and formatted. The final version may differ from this version.

Fig.3

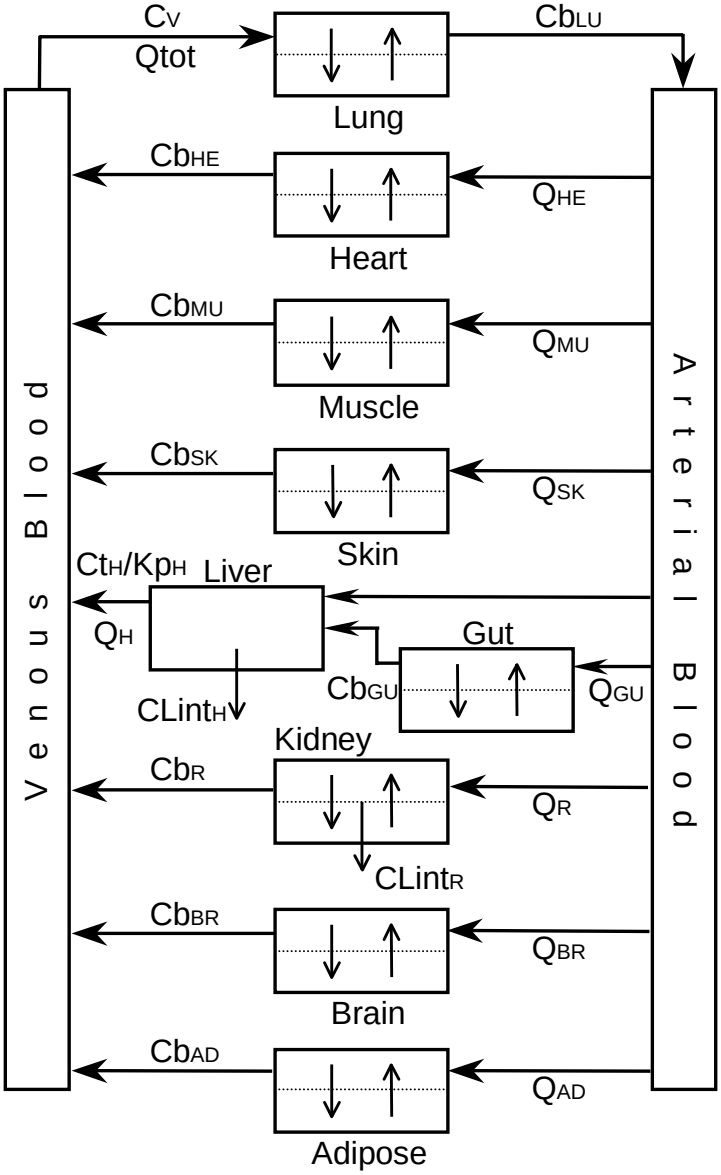

DMD Fast Forward. Published on July 20, 2005 as DOI: 10.1124/dmd.104.001040
This article has not been copyedited and formatted. The final version may differ from this version.

Fig.4

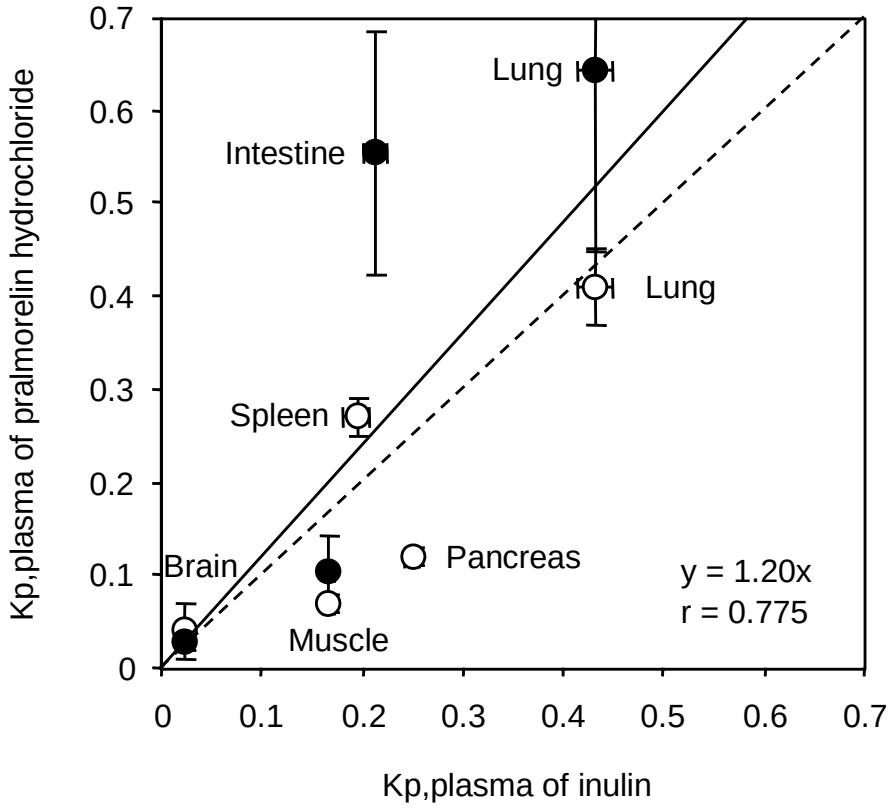

DMD Fast Forward. Published on July 20, 2005 as DOI: 10.1124/dmd.104.001040
This article has not been copyedited and formatted. The final version may differ from this version.

Fig.5

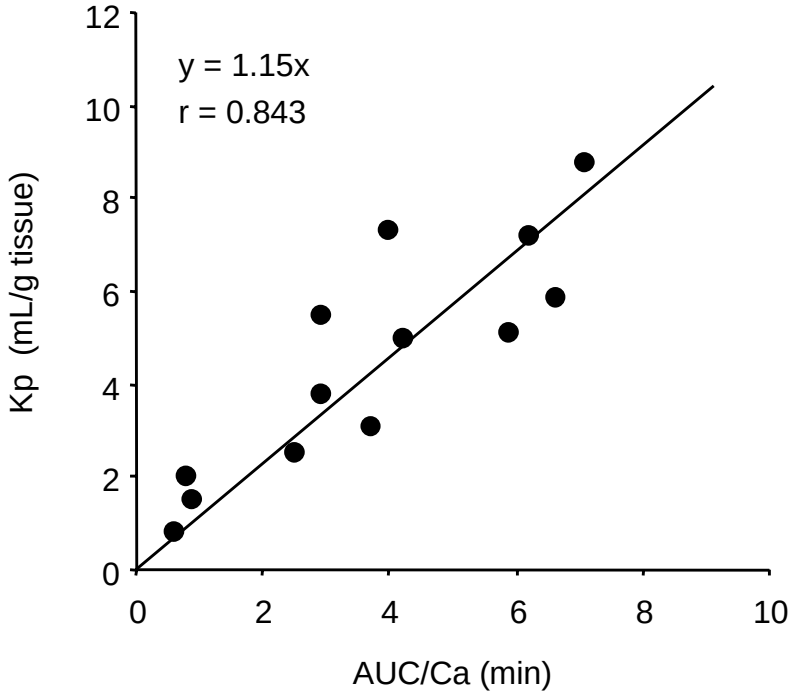

DMD Fast Forward. Published on July 20, 2005 as DOI: 10.1124/dmd.104.001040
This article has not been copyedited and formatted. The final version may differ from this version.

Fig.6

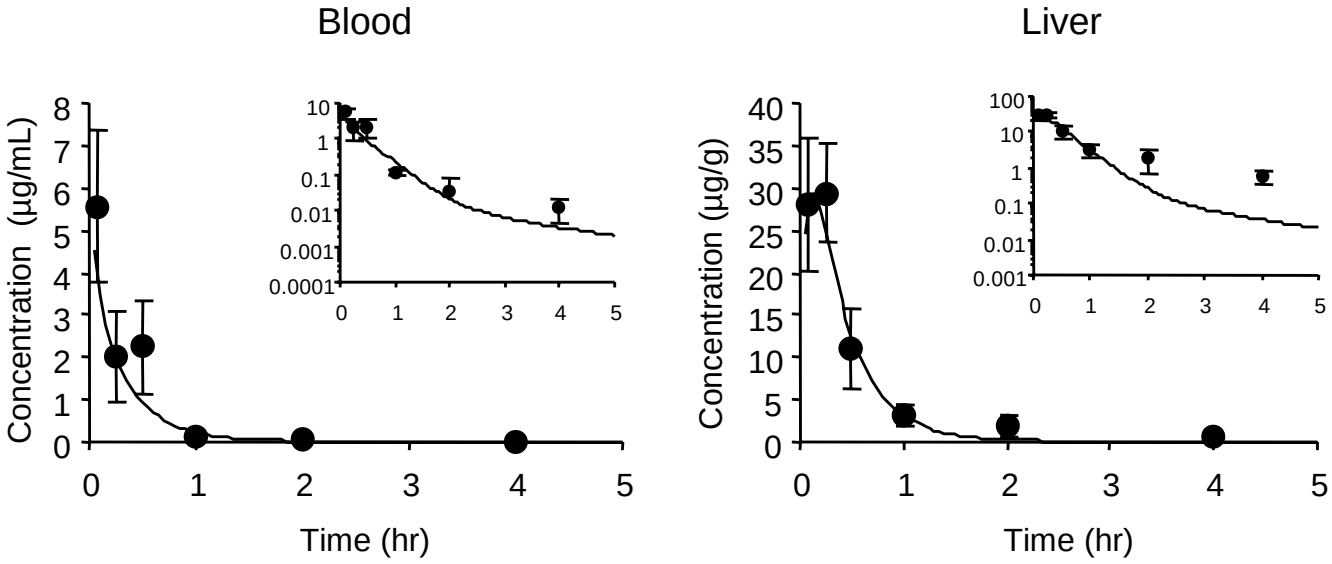

DMD Fast Forward. Published on July 20, 2005 as DOI: 10.1124/dmd.104.001040
This article has not been copyedited and formatted. The final version may differ from this version.

Fig.7

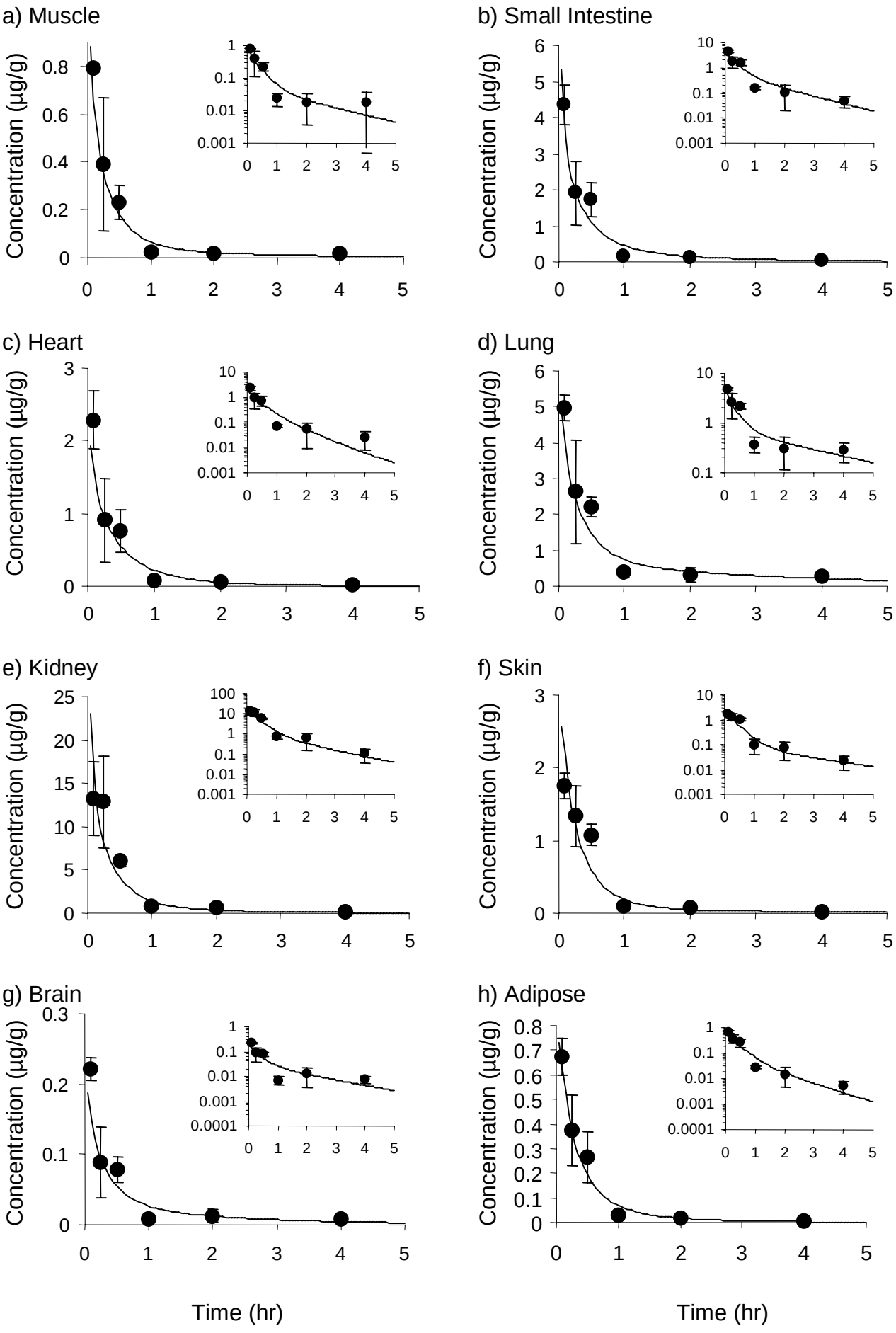

DMD Fast Forward. Published on July 20, 2005 as DOI: 10.1124/dmd.104.001040
This article has not been copyedited and formatted. The final version may differ from this version.

Appendix

Differential Mass Balance Equations for the PB-PK Model

Qt and Vwt represent the blood flow rate and the tissue weight, respectively. Ct, Ca, Cv, Cb are the pralmorelin concentrations in the tissue, arterial blood, venous blood and capillary bed, respectively. Kpss and fb represent the tissue-to-blood partition coefficient and the unbound fraction of pralmolin. LU, HE, MU, SK, H, GU, R, BR, AD represent lung, heart, muscle, skin, liver, small intestine, kidney, brain and adipose tissue, respectively. CLint is the intrinsic clearance.

Arterial blood

$$Va\frac{dCa}{dt} = Qtot \bullet (Cb_{LU} - Ca) \qquad \text{(A1)}$$

Venous blood

$$Vv\frac{Cv}{dt} = \sum Q_{T,i} \bullet Cb_{T,i} + Q_H \bullet Ct_H / Kpss_H - Qtot \bullet Cv \qquad \text{(A2)}$$

Pralmorelin concentrations in tissues with blood flow-limited uptake

(i) Eliminating tissue (Liver)

$$Vwt_H\frac{dCt_H}{dt} = (Q_H - Q_{GU}) \bullet Ca + Q_{GU} \bullet Cb_{GU} - Q_H \bullet Ct_H / Kpss_H - fb \bullet Ct_H \bullet CL_{\text{int}H} / Kpss_H$$

(A3)

where Q_H is the sum of the hepatic artery and portal vein blood flow rates.

Pralmorelin concentrations in tissues with permeability-limited uptake

(i) Lung

DMD Fast Forward. Published on July 20, 2005 as DOI: 10.1124/dmd.104.001040
This article has not been copyedited and formatted. The final version may differ from this version.

$$(Kp_{0LU} \bullet Vwt_{LU}) \frac{dCb_{LU}}{dt} = Qtot \bullet (Cv - Cb_{LU}) - PS_{LU} \bullet fb \bullet Cb_{LU} + k2 \bullet Ct'_{LU} \bullet Vwt_{LU} \quad \text{(A4)}$$

$$Vwt_{LU} \frac{dCt'_{LU}}{dt} = PS_{LU} \bullet fb \bullet Cb_{LU} - k2 \bullet Ct'_{LU} \bullet Vwt_{LU} \quad \text{(A5)}$$

$$Ct_{LU} = Ct'_{LU} + Cb_{LU} \bullet Kp_{0LU} \quad \text{(A6)}$$

(ii) Noneliminating tissues

$$(Kp_{0T} \bullet Vwt_T) \frac{dCb_T}{dt} = Q_T \bullet (Ca - Cb_T) - PS_T \bullet fb \bullet Cb_T + k2 \bullet Ct'_T \bullet Vwt_T \quad \text{(A7)}$$

$$Vwt_T \frac{dCt'_T}{dt} = PS_T \bullet fb \bullet Cb_T - k2 \bullet Ct'_T \bullet Vwt_T \quad \text{(A8)}$$

$$Ct_T = Ct'_T + Cb_T \bullet Kp_{0T} \quad \text{(A9)}$$

(iii) Eliminating tissue (Kidney)

$$(Kp_{0R} \bullet Vwt_R) \frac{dCb_R}{dt} = Q_R \bullet (Ca - Cb_R) - (PS_R + GFR) \bullet fb \bullet Cb_R + k2 \bullet Ct'_R \bullet Vwt_R \quad \text{(A10)}$$

$$Vwt_R \frac{dCt'_R}{dt} = PS_R \bullet fb \bullet Cb_R - k2 \bullet Ct'_R \bullet Vwt_R \quad \text{(A11)}$$

$$Ct_R = Ct'_R + Cb_R \bullet Kp_{0R} \quad \text{(A12)}$$

where $Kp_0 \bullet Vwt$ represents the distribution volume that consists of the blood space and the volume in rapid equilibrium with blood, the concentration in which is equal to Cb. The concentration in the whole tissue (Ct) is given as the sum of the concentration in the intracellular space (Ct') and $Cb \bullet Kp_0$ (Equations A6, A9, A12).